RAPID COMMUNICATIONS

PHYSICAL REVIEW A VOLUME 45, NUMBER 7 1 APRIL 1992

Two-dimensional representation of a delayed dynamical system

F. T. Arecchi,* G. Giacomelli, A. Lapucci, and R. Meucci

Istituto Nazionale di Ottica, Largo E. Fermi 6, 50125 Firenze, Italy

(Received 31 July 1991; revised manuscript received 10 December 1991)

A nonlinear system with delayed feedback, whenever the delay time is much longer than the intrinsic correlation time, displays two widely separated time scales. In such a case, a two-dimensional representation becomes appropriate, because it discloses features otherwise hidden in the one-dimensional sequence of data, and allows use of recognition algorithms developed for spatiotemporal chaos. As an illustration, chaotic time sequences from a single-mode laser with delayed feedback are analyzed using this representation.

PACS number(s): 42.50.Tj, 05.45.+b

In the past decade, successful methods have been introduced and exploited for quantitative characterization of low-dimensional chaos [1]. There is also active investigation of high-dimensional chaos, such as that found in fluid turbulence [2]. In nonlinear optics the transition to high-dimensional chaos, corresponding to the interplay of a large number of degrees of freedom, is realized either by letting many modes compete in an optical resonator [3] or by introducing a delayed feedback [4]. The former case corresponds to the nonlinear interaction of a field at different points in the space-time continuum, and suitable pattern-recognition methods already established for fluid investigation can be used. In the latter case, we deal with a long one-dimensional string of data. Whenever they can be organized on a two-dimensional domain, some hidden features of the complex dynamics appear explicitly as suitable patterns.

In the case of the numerical treatment of a model system, this processing consists in considering the time variable under two different meanings, namely, as a continuous variable confined within a bounded range of size τ where τ is the delay, and as an independent discrete unbounded variable which steps by integer values and counts how many delay intervals run in the course of the system evolution [5]. In a more recent model approach, by regarding the delay-differential (DD) equation as a discretized mapping rule from a "spatial" pattern at time n to a pattern at the delayed time $n+1$, Ikeda and Matsumoto [6] wrote their DD variable as a space-time field, where the space is confined within a delay τ and the time steps by integer values.

In this paper we make use of an equivalent two-dimensional representation to organize the data provided by an experimental system with DD dynamics. This data reorganization sheds light on two nontrivial types of correlations.

The experimental system consists of a single-mode CO_2 laser with an intracavity loss modulation driven by a signal proportional to the output laser intensity. In the feedback loop from the detector to the modulator we insert a delay line and an amplifier. Keeping the feedback amplifier at a constant gain, the control parameters are the delay time τ and the bias voltage B applied at the second input of the feedback amplifier. For a layout of the experiment we refer to Fig. 1 of Ref. [7]. We have initially explored this experimental configuration with no delay [8]. The corresponding single-mode laser dynamics was studied for a wide range of control parameters. In particular a chaotic regime called Shil'nikov chaos has been extensively explored [8(a)]. The chaotic laser intensity had a correlation time T_c of a few tens of microseconds. When we insert a delay around 5 μs, that is, much shorter than the correlation time T_c, a new bifurcation route appears, via two incommensurate frequencies and successive breaking of the two-torus [7]. However, the emerging chaos is still of low dimension and the correlation time remains less than 100 μs, thus, it is intrinsic to the laser dynamics and not dependent on the delay.

Here we investigate what happens when we insert a delay $\tau=1400$ μs, that is, 10 times longer than T_c. Figure 1 shows a few time sequences of the output intensity at different settings of the bias B, digitized with a sampling rate of 1024 data per delay unit. Increasing the B values we observe different dynamical behaviors with pulse shapes resembling those characteristic of the laser without delay [8]. Namely, in Fig. 1(a) a simple oscillation is reported. In Figs. 1(b) and 1(c) successive chaotic behaviors are shown. Figure 1(d) reports a locked situation with pulses slightly different from one another but repeating exactly after one delay period. The display window is about one-half the delay time. The chaotic sequences are generic, and there is no apparent recursivity due to the delay time, as shown in Fig. 1(e) where we plot the chaotic situation already given in Fig. 1(c), but extended over three delay times.

By measuring the time correlation over long times another feature appears. While the correlation function decays over a T_c varying over tens of microseconds, depending on B, it has a revival after a time τ. This means that starting from any data point, the correlation with a point separated by a time distance τ is much larger than the correlation with a closer point (separated by, say, one-tenth of τ). In such a case, the interplay of nonlinearity and delay implies two different relevant time scales.

The autocorrelation function of the signal presented in Figs. 1(c) and 1(e) has been calculated over 16384 time data and reported in Fig. 2. In the upper part it is evident

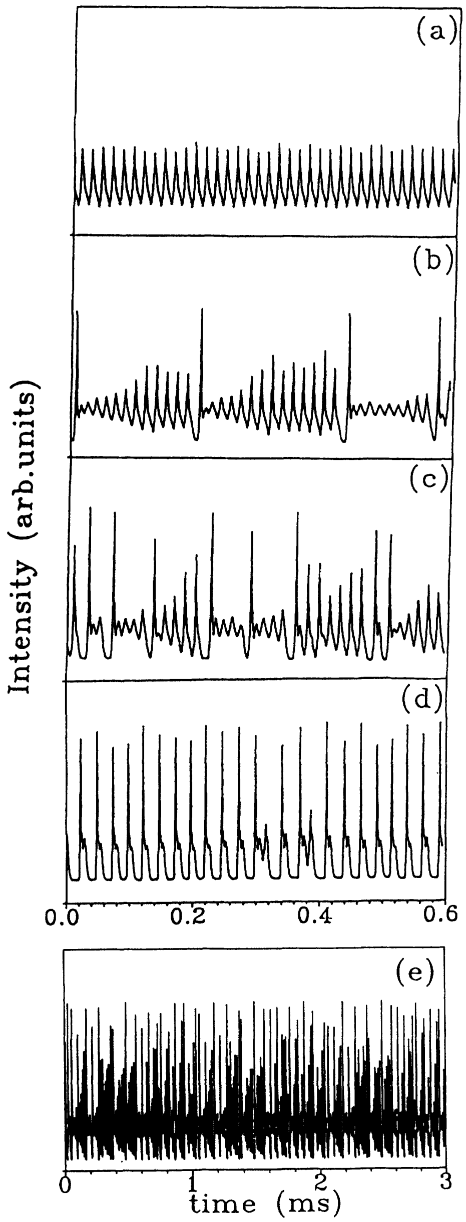

FIG. 1. Output laser intensity vs time for four increasing values of the bias B. (a) Regular oscillations; (b),(c) chaotic behaviors; (d) quasiregular pulsing. (e) Same as case (c) but over a large time range. In the following figures we elaborate on the same four cases as (a)–(d).

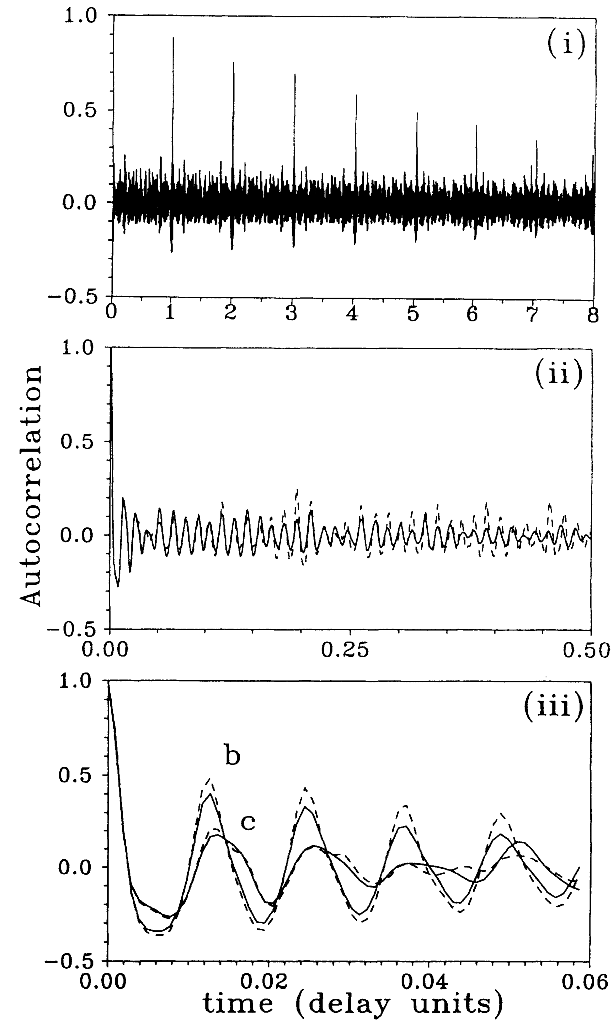

FIG. 2. Autocorrelation functions of the laser intensity fluctuations. Horizontal scale: time in delay units. (i) Autocorrelation function over a time interval of several delay units. (ii) Autocorrelation functions within a delay unit τ, averaged over many consecutive delays (solid line) for the same signal of Fig. 1(c). For comparison, the first unit of (i) is expanded to the same scale and superposed (dashed lines) to show the difference between the ensemble-averaged and the time-averaged correlation functions. (iii) Expanded version of (ii) including the ensemble- and time-averaged correlation functions of Fig. 1(b). Up to a time equal to 0.1 delay units, there is a fair agreement between solid- and dashed-line plots.

the quasiperiodic behavior, with revivals at each delay unit τ and a slow decay over several (about 10) τ units. The central part of the figure shows that, within a single delay unit, the correlation function decays over tens of microseconds. This short decay is intrinsic to the nonlinear dynamics. Indeed, for the same B parameter, it has the same value as with no delay [8] or with a short delay [7]. In fact, the decay rate of the population inversion is around $10^4\ s^{-1}$ and it coincides with the decay rate of the correlation in a linearized model [8(b)]. The plot given in dashed lines is an expansion of the first delay unit of the upper figure. The solid line corresponds to averaging over 500 delay units as if they were different samples of a statistical ensemble. Notice that the two plots show sizable differences; however, the first part over which the decay time is evaluated is not modified by the ensemble averaging, as shown in the further expansion in the lower part of Fig. 2. Here we have also added the autocorrelation for the signal of Fig. 1(b). The short-time overlap of dashed and solid lines shows that the correlation time scale is indeed independent of the delay, thus suggesting that the data points depend on two separate variables rather than on a single one.

A two-dimensional reorganization of the data closely follows the numerical technique which solves DD equations [5]. The state of a DD equation such as

$$\dot{x}(t)=F(x(t),x(t-\tau)) \tag{1}$$

is determined by all the values of the function x in the interval $(t, t-\tau)$. This function can be approximated by N samples taken at intervals $\Delta t=\tau/(N-1)$. The evolution consists of an N-dimensional discrete mapping. Choosing the Euler integration scheme for Eq. (1), that is,

$$x(t+\Delta t)=x(t)+F(x(t),x(t-\tau))\Delta t\,, \tag{2}$$

the N-dimensional mapping is defined by the generic term [5]

$$x_s(k+1)=x_{s-1}(k)+F(x_{s-1}(k+1),x_s(k)) \tag{3}$$

where we have denoted by s an index ranging from 1 to N and corresponding to a single delay interval, and by k a discrete index counting the delay units. Equation (3) is completed by two slightly different equations at the boundaries $s=1$ and $s=N$, as shown in Ref. [5].

The above procedure suggests an organization of the data in a two-dimensional "space-time" domain $s-k$, where the space cell corresponds to a single delay and the unbounded time is spanned in terms of delay units.

As long as $\tau < T_c$, all points along the s axis are strongly correlated and hence the two-dimensional representation is a pure visualization of the technique leading to Eq. (2) but it does not bring any physical insight. In contrast, when $\tau \gg T_c$ the points along the s axis decorrelate, and then the correlation revives after τ, as indicated by Eq. (3), yielding a nontrivial two-dimensional representation. An organization of data along these lines (Fig. 3) shows indeed a cellular structure as in space-time turbulence [9]. This two-dimensional reorganization looks similar to that already reported for mode-locked laser pulses [10]. Also in Ref. [10] the two-dimensional representation was motivated by recursive relations as in our case. However, in that treatment the role of our correlation time T_c is played by the finite pulse duration. This means that there is no signal overlap beyond a time unit, and thus no build up of long-range interactions as in our case.

Putting a threshold at 0.3 of the maximum pulse height, we obtain (Fig. 4) a digitized space-time picture in black (above threshold) and white (below threshold) for the same four experimental cases which were represented as one-dimensional strings in Fig. 1. The two-dimensional representation provides a visual discrimination among the different types of chaotic behavior. This discrimination is much more evident than the one-dimensional representa-

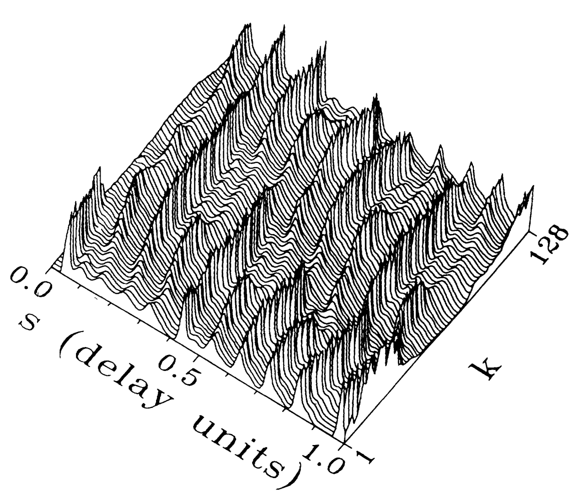

FIG. 3. Cellular pattern obtained by plotting the signal $x(s,k)$ vs s $(0<s<\tau)$ for successive k. The data refer to the parameter values of Fig. 1(c). The decay of the correlations along s occurs over a time T_c (around 0.1 delay units) while along k correlations last for tens of delay units. Notice that in the case $\tau \ll T_c$ of Ref. [7] this cellular representation would have trivially provided parallel rolls, uniform along the space direction s.

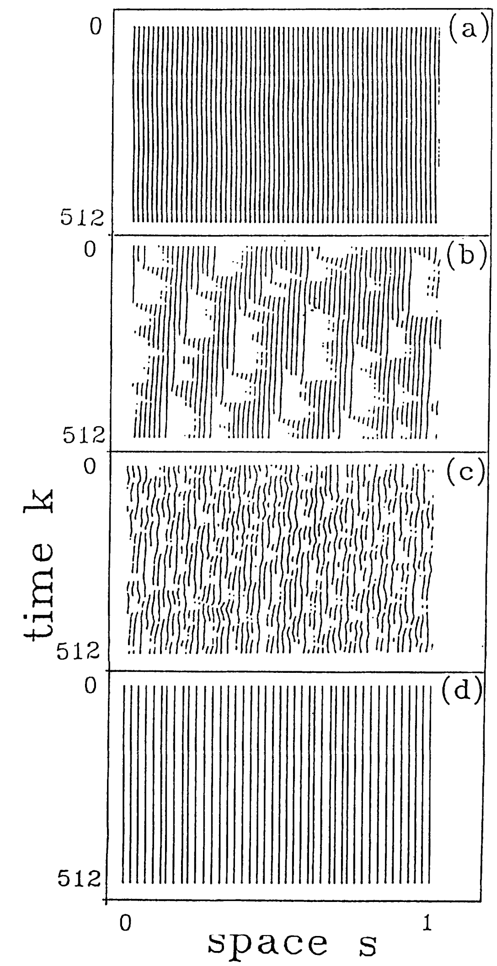

FIG. 4. Two-dimensional representations of the laser signals shown in Fig. 1. The plots are obtained putting a threshold at 0.3 of the maximum data value. The horizontal axis ranges over one delay unit while the vertical axis covers 512 delay units. The black regions correspond to data above the threshold and white regions to data below the threshold. Panels (b) and (c) show chaotic behaviors with different two-dimensional patterns. Panel (d) corresponds to a locked regime consisting of irregular pulse locations in the spatial direction but repeating after one delay, hence strongly correlated in the temporal direction. In this representation, they appear as dislocations of a lattice.

tion of Fig. 1. Indeed it is directly observable that patterns like b and c have "cellular structures" which decorrelate rapidly both along k and s.

Notice that in Fig. 4(b) we obtain triangular features resembling those generated by cellular automata [11]. Indeed our recursive relation (3) is a coupling among sites which differ by both space and time, and furthermore the binary patterns of Fig. 4 have reduced the continuous dynamics to a two-state dynamics. Thus binary plots like Fig. 4 permit a model of a given experimental dynamics by a suitable cellular automaton.

The two-dimensional representation here introduced allows extraction of quantitative indicators, with more detailed information than that provided by the binary plots of Fig. 4. In doing this, we can exploit the indicators introduced for space-time phenomena as, e.g., the space-time correlation functions of the signal $x(s,k)$ in Fig. 3, or the mutual information maps as introduced in Ref. [6]. The limited experimental resolution and length of data records are not yet sufficient for a reliable evaluation of Lyapunov spectra as done in numerical solutions of coupled-map lattices [12].

A presentation of these space-time indicators for a delayed system will be reported elsewhere.

*Also at Dipartimento di Fisica, Università degli Studi di Firenze, I-50125 Firenze, Italy.

[1] See, e.g., *Dimensions and Entropies in Chaotic Systems,* edited by G. Mayer-Kress (Springer-Verlag, Berlin, 1986).

[2] See, e.g., *Advances in Fluid Turbulence,* edited by G. Doolen, R. Ecke, D. Holan, and V. Steinberg [Physica D **37**, Nos. 1-3 (1989)]; and *Measures of Complexity and Chaos,* edited by N. B. Abraham, A. M. Albano, A. Passamante, and P. E. Rapp (Plenum, New York, 1990).

[3] F. T. Arecchi, G. Giacomelli, P. L. Ramazza, and S. Residori, Phys. Rev. Lett. **65**, 2531 (1990).

[4] K. Ikeda and K. Matsumoto, Physica D **29**, 223 (1989).

[5] J. D. Farmer, Physica D **4**, 366 (1982).

[6] K. Ikeda and K. Matsumoto, Phys. Rev. Lett. **62**, 2265 (1989).

[7] F. T. Arecchi, G. Giacomelli, A. Lapucci, and R. Meucci, Phys. Rev. A **43**, 4997 (1990).

[8] (a) F. T. Arecchi, A. Lapucci, R. Meucci, J. A. Roversi, and P. H. Coullet, Europhys. Lett. **6**, 677 (1988); (b) F. T. Arecchi, W. Gadomski, A. Lapucci, H. Mancini, R. Meucci, and J. A. Roversi, J. Opt. Soc. Am. B **5**, 1153 (1988).

[9] B. I. Shraiman, Phys. Rev. Lett. **57**, 325 (1987).

[10] G. H. C. New and J. M. Catherall, in *Optical Instabilities,* edited by R. W. Boyd, M. G. Raymer, and L. M. Narducci (Cambridge Univ. Press, Cambridge, England, 1985), p. 197.

[11] S. Wolfram, *Theory and Applications of Cellular Automata* (World Scientific, Singapore, 1986).

[12] K. Kaneko, Physica D **23**, 436 (1986).